# Accurate surface potential determination in Schottky diodes by the use of a correlated current and capacitance voltage measurements. Application to n-InP

Ali Ahaitouf[1, †], Abdelaziz Ahaitouf[2], Jean Paul Salvestrini[3], and Hussein Srour[3]

[1]Laboratoire Signaux Systèmes et Composants, DGE Faculty of Sciences and Technology, Université Sidi Mohammed Ben Abdellah, P. O. Box 2202, FES Morocco
[2]LIMAO Faculté polydisciplinaire de Taza, Université Sidi Mohammed Ben Abdellah de Fés, BP 1223 Taza-Gare, Morocco
[3]Laboratoire Matériaux Optiques, Photonique et Systèmes, EA 4423, Université Paul Verlaine-Metz, Supélec, 2 rue E. Belin, 57070 Metz, France

**Abstract:** Based on current voltage ($I$–$V_g$) and capacitance voltage ($C$–$V_g$) measurements, a reliable procedure is proposed to determine the effective surface potential $V_d$ ($V_g$) in Schottky diodes. In the framework of thermionic emission, our analysis includes both the effect of the series resistance and the ideality factor, even voltage dependent. This technique is applied to n-type indium phosphide (n-InP) Schottky diodes with and without an interfacial layer and allows us to provide an interpretation of the observed peak on the $C$–$V_g$ measurements. The study clearly shows that the depletion width and the flat band barrier height deduced from $C$–$V_g$, which are important parameters directly related to the surface potential in the semiconductor, should be estimated within our approach to obtain more reliable information.

**Key words:** Schottky diode; interface states; surface potential; ideality factor; barrier height; capacitance voltage; current measurements

**DOI:** 10.1088/1674-4926/32/10/104002 **EEACC:** 2560

## 1. Introduction

Schottky diodes are one of the most widely used devices in the development of modern electronics. Electrical characterizations of these kinds of structures are generally considered as figures of merit for devices before their final fabrication. The determination of Schottky diodes parameters has always been an exciting debate and still gives rise to publications[1−15].

A consistent technique for barrier height determination is thus of a high importance for Schottky diode characterization. Schottky diode parameters, which are barrier height, series resistance, ideality factor, doping concentration[16] and even interface states[16−18], are usually deduced from ($I$–$V_g$) and/or ($C$–$V_g$) measurements analysis. Nevertheless, depending on the kind of analysis used [($I$–$V_g$) or ($C$–$V_g$)], the barrier height values obtained for a given structure can be quite different[16]. We will show in this paper that this originates from an inexact knowledge of the real diffusion potential and that a more accurate determination of this voltage leads to a more reliable barrier height value especially deduced from $C$–$V_g$. In fact, our rigorous procedure enables us to obtain the whole distribution of the surface potential in the structure taking into account separately both the series resistance and the ideality factor. This distribution of surface potential constitute an immediate and clear indication of the surface voltage modulation by the bias, which is directly related to the quality of the interface between the metal and the semiconductor. Moreover, the knowledge of the real surface potential value is essential for the characterization of the depletion layer, which plays an important role in devices such as photodetectors, high electron mobility transistors and metal semiconductor field effects transistors.

Our approach will be used with indium phosphide (InP), a direct band gap III–V semiconductor, which is a potential candidate for many applications such as MESFET devices, microwave and infrared detectors, frequency converters and other optoelectronic devices[19−21]. It has been widely studied for use in Schottky diodes. Their development was seriously impeded by a low Schottky barrier height, around 0.45 eV[16]. To increase this barrier value, many methods have been proposed, among which sulfur passivation[17−22] and the growth of a controllable thin oxide layer were used as a tool for surface passivation and improvement of characteristic[23−25].

We will also show that using our approach, the so-called anomalous peak in the $C$–$V_g$ measurements, which has been attributed to many and different origins (including ohmic contact nature[1], series resistance and interface states[27] or the non-validity of the depletion layer model[8]), is observed when the flat band conditions are not yet reached, unlike it is claimed in many works[1−6]. Finally, our approach shows that, among the different origins of the $C$–$V_g$ peaks proposed in the literature, the interface states appear to play the dominant role.

## 2. Theoretical background and procedure

Schottky diode capacitance is usually described according to the depletion approximation[16] by the well known expression:

$$C = \sqrt{\frac{\epsilon_o \epsilon_{sc} q N_D}{2\,|V_d|}}, \tag{1}$$

† Corresponding author. Email: ali_ahitouf@yahoo.fr
Received 21 January 2011, revised manuscript received 14 June 2011

where $\epsilon_o$ and $\epsilon_{sc}$ denote, respectively, the dielectric permittivity of vacuum and of the semiconductor (SC), $q$ is the electronic charge, $N_D$ is the doping concentration of the semiconductor and $V_d$ denotes the surface potential of the SC.

The current–voltage characteristic for a Schottky diode is given by[16]:

$$I = AA^*T^2 \exp\left(-\frac{q\phi_{bo}}{kT}\right) \exp \frac{q(V_g - R_sI)}{nkT} \times \left\{1 - \exp\left[-\frac{q(V_g - R_sI)}{kT}\right]\right\}. \quad (2)$$

This equation describes the thermionic emission current[16] and is generally used to analyze current measurements of Schottky diodes. In this expression, $A$ is the effective diode area, $A^*$ is the modified Richardson constant, $\phi_{bo}$ is the Schottky barrier height at zero bias voltage, $V_g$ is the bias voltage, $n$ is the ideality factor and $R_s$ denotes the series resistance. $T$ and $k$ correspond respectively to the absolute temperature and the Boltzmann constant.The term $\frac{V_g - R_sI}{n}$ in Eq. (2) corresponds to the amount of surface potential variation in the SC[10] leading to the effective surface voltage in the SC:

$$V_d = -V_{do} + \frac{V_g - R_sI}{n}, \quad (3)$$

where $V_{do}$ is the built-in voltage. Generally, the value of the ideality factor $n$ is obtained considering the slope of the straight line in the semilogarithmic forward $I$–$V_g$ plot for $V_g \geqslant \frac{3kT}{q}$. Nevertheless, due to the presence of interface states, see for instance references[12, 17, 18], $n$ is generally voltage dependent. In this case, it is necessary to obtain the value of $n$ for each bias voltage by using the following equation derived from Eq. (2):

$$n = \frac{q}{kT} \frac{\left[1 - R_s\left(\frac{\partial I}{\partial V_g}\right)\right] \partial V_g}{\partial \ln \frac{I}{1 - \exp\left[-\frac{q(V_g - R_sI)}{kT}\right]}}. \quad (4)$$

Finally, the real effective surface voltage as expressed in Eq. (3) becomes for each bias voltage $V_g$:

$$V_d = -V_{do} + \frac{V_g - R_sI(V_g)}{n(V_g)}. \quad (5)$$

Knowing the exact value of the diffusion potential, the flat band barrier height $\phi_{bc}$ is then calculated using the standard equation:

$$\phi_{bc} = V_{do} + \frac{kT}{q} \ln \frac{N_c}{N_D} + \frac{kT}{q}, \quad (6)$$

where $N_c$ denotes the effective density of states in the conduction band.

To get the whole set of parameters characterizing a Schottky diode, we use the following procedure. The series resistance $R_s$ and the mean ideality factor values are deduced from $I$–$V$ measurements by using the following Cheung and Cheung function[11]

$$\frac{dV_g}{d(\ln I)} = R_sI + \frac{nkT}{q}. \quad (7)$$

Table 1. Chemical treatments of the samples.

| Sample | Alcohol | HCl | $(NH_4)_2S$ | Annealing | UV oxidation |
|---|---|---|---|---|---|
| A | | x | x | x | |
| B | | x | | | |
| C | x | | | | x |

The plot of Eq. (7) yields the determination of the value of $R_s$ via the slope of the corresponding curve. The value of $n\frac{kT}{q}$ is deduced from the intercept on the $y$ axis. In addition to the confirmation of the value of $R_s$ derived from Eq. (7), the second function of Cheung and Cheung[11] which is:

$$H(I) = V_g - n\frac{kT}{q} \ln \frac{I}{AA^*T^2} = V_g - n\phi_{bo}, \quad (8)$$

leads to the determination of the zero bias barrier height.

The ideality factor $n(V_g)$ is derived according to Eq. (4). The built-in voltage $V_{do}$ is equal to the voltage value $V_{go}$ obtained using $C$–$V_g$ measurements by extrapolating the plot of $1/C^2$ versus $V_g$ to the voltage axis. Finally, using the deduced parameters ($R_s$, $n(V_g)$ and $V_{do}$), the theoretical $C$–$V_g$ curve is compared to the experimental one in order to check the reliability of the obtained values for each parameter.

## 3. Results and discussion

### 3.1. Experimental details

All of the Schottky structures considered here are realized on an involuntary n-type (100) InP substrate, with a nominal carrier concentration of $N_D = 5 \times 10^{15}$ cm$^{-3}$ supplied by Crismatec InPact. They will be referred as A, B and C in the following as described in Table 1. Samples A and B have been etched in hydrochloric acid (HCl) (3 mol/L) for 5 min to remove native oxide and quickly rinsed in deionized water. Sample A has then been immersed in a 50 ℃ heated ammonium sulfur solution $(NH_4)_2S$ with a concentration of 0.5 mol/L for 20 min and cleaned in deionized water and finally annealed at 300 ℃ under 3 mbar nitrogen ($N_2$) ambiance during 30 min. This sulfur treatment has been used to passivate the InP surface[17].

The third sample (C) is an epi-ready UV oxidized structure with a 1.2 nm oxide thickness and has been only degreased in alcohol and not submitted to any further chemical treatments. Circular gold dots of $6.36 \times 10^{-3}$ cm$^{-2}$ have been deposited by thermal evaporation under a vacuum pressure of $10^{-6}$ mbar on polished surface of all the samples. The ohmic contact was realized by thermal evaporation of gold germanium eutectic followed by a protective gold layer on the rear of the substrates.

### 3.2. Results and discussion

Current and capacitance measurements $I$–$V_g$ and $C$–$V_g$ have been carried out using a source measure unit (SMU) Keithley 236 and a HP4280A 1-MHz capacitance meter. Equation (7) and (8) are used to obtain the series resistance $R_s$, the average ideality factor n and the apparent barrier height $\phi_{bo}$ of the Schottky contact. Table 2 summarizes all the characteristics deduced from $I$–$V_g$ measurements. The weakest values of $R_s$ and $n$ are obtained for the sulfur-treated sample A. Sample

Table 2. Parameters as deduced from $I$–$V_g$ and $C$–$V_g$ measurements; $R_s$ denotes the series resistance, $n$ the ideality factor, $\phi_{bo}$ the zero bias barrier height, $V_{do}$ the diffusion potential, $N_D$ the doping density, $\phi_{bc}$ the flat band barrier height and $\phi_{bcc}$ the corrected value of $\phi_{bc}$.

| Sample | $I$–$V$ measurements | | | | $C$–$V$ measurements | | |
|---|---|---|---|---|---|---|---|
| | $R_s$ (Ω) | $n$ | $\phi_{bo}$ (eV) | $V_{do}$ (V) | $N_D$ ($10^{15}$ cm$^{-3}$) | $\phi_{bc}$ (eV) | $\phi_{bcc}$ (eV) |
| A | 14.7 | 1.12 | 0.59 | 0.523 | 4.15 | 0.674 | 0.62 |
| B | 26.5 | 1.35 | 0.53 | 0.643 | 4.63 | 0.792 | 0.625 |
| C | 86 | 1.9 | 0.59 | 0.895 | 9.5 | 1.025 | 0.6 |

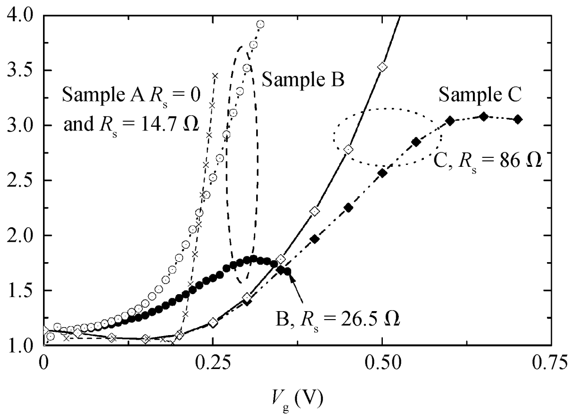


Fig. 1. Ideality factor $n$ versus voltage for samples A, B and C, with and without taking into account the value of $R_s$. For sample A, the two curves are superimposed due to the very small value of $R_s$.

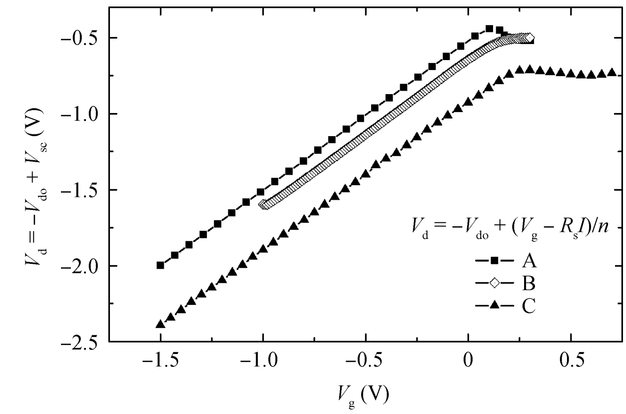


Fig. 2. Surface potential characteristic versus voltage for all samples.

B shows larger values of $R_s$ and $n$ due probably to the presence of an involuntary oxide layer[17]. The highest values of $R_s$ and $n$ correspond to the UV oxidized sample. With regard to the barrier heights, for sample A the obtained value indicates a beneficial effect of sulfur treatments whereas for samples B and C the obtained values, even if they are higher than the value of 0.45 eV reported for the intimate metal contact on n-InP[16], must be considered carefully because of the interfacial layers and the relatively large values of $R_s$.

As discussed above, the ideality factor $n$ depends on $V_g$. These dependences are determined for each sample by using Eq. (4) and the results are reported on Fig. 1. We can note that, for sample A, $n$ approaches 1 up to $V_g = 0.2$ V and then increases monotonically for higher voltages. For samples B and C, $n$ increases with voltage from 1 up to a maximum around $V_g = 0.3$ V and $V_g = 0.6$ V respectively for the two samples. These peaks can be entirely hidden if we do not take into account the value of series resistance (see the dashed curves on Fig. 1 for $R_s = 0$ Ω). The peaks in the $n$ versus voltage curve are attributed to an interface states effect, as previously reported for oxidized Schottky diodes[17, 18] and as observed for sample A after prolonged air exposure[17]. From Fig. 1 we can also notice that the effect of series resistance becomes important only beyond a given value of $V_g$ depending on the structure, which is respectively equal to 0.13 and 0.3 V for samples B and C.

We have also used the experimental data of $C$–$V_g$ measurements, to determine the diffusion potential $V_{do}$, the flat band barrier $\phi_{bc}$ as well as the doping density from the slope of the $1/C^2 = f(V_g)$ plot. Table 2 shows the results. The doping density values obtained for samples A and B are in good agreement with those indicated by the manufacturer. For sample C, the value deduced from our measurements is larger than the nominal one. The values of $\phi_{bc}$ for all the samples do not agree with those deduced from $I$–$V_g$ measurements. This large difference could originate from an overestimation of the values of the built-in voltage $V_{do}$ deduced by extrapolating the $1/C^2 = f(V_g)$ plot. In fact, when considering non-ideal structures, the value of $V_{do}$ should be corrected by taking into account the ideality factor as indicated by Eq. 3 and as reported by Türüt *et al.*[26]. Assuming the average value of $n$ given in Table 2, we have recalculated the barrier height value $\phi_{bcc}$. The new values, reported in Table 2, seem to be more reliable since they are in good agreement with those initially deduced from $I$–$V_g$ measurements. This could also explain the high value of the doping density obtained for sample C. In this case the slope of the $1/C^2 = f(V_g)$ plot is proportional to $\frac{1}{n} \times \frac{1}{N_D}$. Thus taking into account this correction, the new value of $N_D$ is found to be equal to $5 \times 10^{15}$ cm$^{-3}$ for sample C, which is in a good agreement with the nominal one.

With regard to the barrier height, it is well known that the current voltage and capacitance voltage measurements give different values with the higher deduced from capacitance measurements. The discrepancies are habitually attributed to the fact that the $I$–$V_g$ gives the zero bias barrier whereas the $C$–$V_g$ give the flat band barrier. Our results show that the flat band condition is difficult to obtain, because when nearing the flat band, the current becomes so important that effects of the series resistance and eventually the pinning of the surface Fermi level by surface states becomes so important that the structure is still slightly depleted (see Fig. 2, below). Our results show that by taking into account the series resistance and ideality factor, which varies with the voltage, the two barrier heights can be quite comparable.

By using Eq. (5), the values of $V_{do}$ (deduced from the plot $1/C^2 = f(V_g)$), $R_s$ and $n(V_g)$, the characteristic $V_d(V_g)$ can

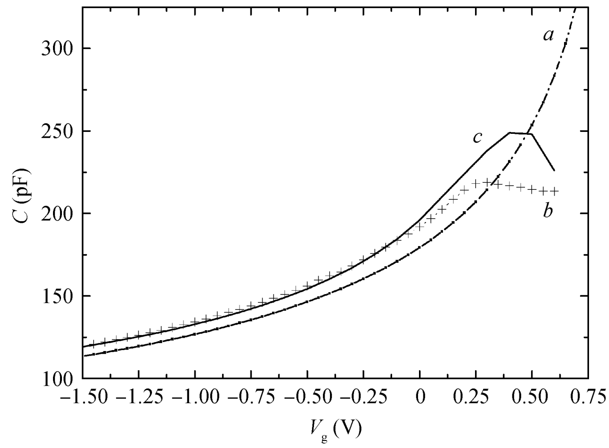


Fig. 3. Comparison between capacitance–voltage characteristics for sample C. (*a*) calculated according to the depletion model, (*b*) from measurements and (*c*) from measurements corrected according to our procedure.

be built for each structure. Theses curves are reported on Fig. 2. For the whole set of curves and for negative values of $V_g$, $V_d$ is increasing linearly and exhibits a plateau-like behavior for positive values of $V_g$. The values of $V_d$ corresponding to the plateau is equal to $-0.5$ V for samples A and B and to $-0.75$ V for sample C. We can note also that the value of $V_g$ corresponding to the beginning of the plateau is shifted to higher values of $V_g$ for the oxidized structure (sample C). These negative values of $V_d$ clearly indicate that the diodes are still reverse biased for this positive range of $V_g$. This pinning, revealed by the plateau of $V_d$, is also observed for sample A even if the value or $R_s$ is small. One can reasonably attribute this behavior to interface state effects that restrict the Fermi level displacement. Indeed the increase of $n$, when the direct bias voltage increases, has been attributed to the motion of the Fermi level into a higher interface states density which is in equilibrium with the SC[9, 27]. For samples B and C, the observed peak in the $n(V_g)$ curve corresponds to a maximum in the interface state distribution for oxidized Schottky structures[17, 18] and are mainly due to the involuntary grown interfacial layer for sample B and the oxide layer for sample C. The distribution and the density of the interface states have been determined from the $n$–$V_g$ curve, confirmed by DLTS measurements[28] and can be mainly responsible for the observed Fermi level pinning.

From theses characteristics we have then calculated, for all samples, the capacitance values for each voltage using Eq. (1). For example, we report in Fig. 3 the calculated and measured curves for sample C. For comparison, we have also reported the theoretical curve as predicted by the depletion model [Eq. (1)]. The calculated curve shows a maximum located at $V_g = 0.3$ V, which is not expected according to Eq. (1). A very good agreement is obtained between the theoretical and experimental curves, especially for negative values of $V_g$ when the structure is in a deeper depletion range. The discrepancies between the calculated and measured capacitances values for positive values of $V_g$ cannot be attributed to a wrong value of $R_s$ since, as we have calculated, the series resistance does not significantly change the behavior of the capacitance curve in this voltage range. However, it can originate from a slightly overestimated $V_{do}$. In fact, according to Eqs. (1) and (5) and with the condition $\frac{1}{C^2} = 0$ (by extrapolation), the built-in voltage $V_{do}$ can be written as:

$$V_{do} = \frac{V_{go}}{n(V_{go})} - \frac{R_s I_o}{n(V_{go})}, \tag{9}$$

where $I_o$ denotes the current corresponding to $V_{go}$. The value of $V_{do}$ deduced according to Eq. (9) can be quite different from $V_{go}$ especially for large values of $R_s$ and $n(V_{go})$ as is the case for sample C. The value of $V_{do}$ in this case is overestimated leading to a smaller calculated value of the capacitance.

Concerning the observed peak on the capacitance measurements, it was reported in Ref. [4] that a broadening of this peak is associated with a decrease of its intensity when $R_s$ increases. Our results do not confirm this interpretation. Indeed it is clear that even in the case of high values of $R_s$, as for sample C, $R_s$ plays a negligible role in the voltage region (0.3 V for sample C) and (0.25 V for sample B and 0.02 V for sample A not shown here) corresponding to the observed peak on the calculated curve. However, its effect appears for higher voltages as shown on Fig. 1 and as reported by Mikhelasvili[15]. We can then conclude that all the observed peaks on the capacitance measurements, for diodes where the thermionic emission is the dominant current transport mechanism mainly originate from interface states effects and cannot be immediately related to series resistance as reported previously[4, 6]. The effect of the series resistance, if the corresponding value is high, appears only for higher voltages far from the maximum capacitance corresponding voltage.

## 4. Conclusion

By using simultaneously the current and capacitance versus voltage measurements, we have proposed a procedure to determine the effective surface potential in the semiconductor. Thus the flat band barrier height deduced from $C$–$V_g$ is in good agreement with the zero bias barrier deduced from $I$–$V_g$ measurements. This approach is validated here for MS-(n)InP structures with and without interfacial layer. We have also analyzed the effect of the series resistance and shown that the capacitance peak appears even if the structure is still in depletion and that its origin can be attributed mainly to interface states density. This contribution shows that the estimation of the depletion layer width as well as the flat band barrier height cannot be made reliably regardless of ideality factor consideration, especially when its value is far from unity, as is the case for most fabricated lab diodes. This study shows that the correlation between $I$–$V_g$ and $C$–$V_g$ measurements is a good way to obtain reliable information about interface properties and is suitable for the large band gap SC thin films diodes.

## Acknowledgement

We would like to thank Professor A. Bath for his help and scientific discussions

## References

[1] Werner J, Levi A F J , Tung R T, et al. Origin of the excess capacitance at intimate Schottky contacts. Phys Rev Lett, 1988, 60:

53
[2] Chattopadhyay P, Raychaudhuri B. Origin of the anomalous peak in the forward capacitance–voltage plot of a Schottky barrier diode. Solid-State Electron, 1992, 35: 875
[3] Chattopadhyay P, Raychaudhuri B. New technique for the determination of series resistance of Schottky barrier diodes. Solid-State Electron, 1992, 35: 1023
[4] Chattopadhyay P, Raychaudhuri B. Frequency dependence of forward capacitance–voltage characteristics of Schottky barrier diodes. Solid-State Electron, 1993, 36: 605
[5] Chattopadhyay P, Sanyal S. Capacitance–voltage characteristics of Schottky barrier diode in the presence of deep-level impurities and series resistance. Appl Surf Sci, 1995, 89: 205
[6] Sahin B, Çetin H, Ayyildiz E. The effect of series resistance on capacitance–voltage characteristics of Schottky barrier diodes. Solid State Commun, 2005, 135: 490
[7] Aydoğan S, Çinar K, Asil H, et al. Electrical characterization of Au/n-ZnO Schottky contacts on n-Si. J. Alloys Compd, 2009, 476: 913
[8] Hjelmgren H, Kollberg E, Lundgren L. Numerical simulations of the capacitance of forward-biased Schottky-diodes. Solid-State Electron, 1991, 34: 587
[9] Card H C, Rhoderick E H. Studies of tunnel MOS diodes: I. Interface effects in silicon Schottky diodes. J Phys, 1971, D4: 1589
[10] Wu C Y. Interfacial layer theory of the Schottky barrier diodes. J Appl Phys, 1980, 51: 3786
[11] Cheung S K, Cheung N W. Extraction of Schottky diode parameters from forward current–voltage characteristics. Appl Phys Lett, 1986, 49: 85
[12] Viktorovitch P, Louis P, Besland M P, et al. Electrical characterization of metal–oxide–InP tunnel diodes based on current–voltage, admittance and low frequency noise measurements. Solid-State Electron, 1995, 38:1035
[13] Ahmad Z, Sayyad M. Extraction of electronic parameters of Schottky diode based on an organic semiconductor methyl-red. Physica E, 2009, E41: 631
[14] Rodrigues A M. Extraction of Schottky diode parameters from current–voltage data for a chemical-vapor-deposited diamond/silicon structure over a wide temperature range. J Appl Phys, 2008, 103: 83708
[15] Mikhelashvili V, Ainsenstein G, Uzdin R. Extraction of Schottky diode parameters with a bias dependent barrier height. Solid-State Electron, 2001, 45: 143
[16] Rhoderick E H, Williams R H. Metal semiconductor contacts. Oxford: Clarendon Press, 1988: 38
[17] Ahaitouf A, Bath A, Losson E, et al. Stability of sulfur-treated n-InP Schottky structures, studied by current–voltage measurements. Mat Sci Eng B, 1998, 52: 208
[18] Maeda K, Ikoma H, Sato K, et al. Current–voltage characteristics and interface state density of GaAs Schottky barrier. Appl Phys Lett, 1993, 62: 2560
[19] Horvath Z J, Rakovics V, Szentpali B, et al. InP Schottky junctions for zero bias detector diodes. Vacuum, 2003, 71: 113
[20] Kazemi H, Shinohara K, Nagy G, et al. First THz and IR characterization of nanometer-scaled antenna-coupled InGaAs/InP Schottky-diode detectors for room temperature infrared imaging. Proc SPIE, 2007, 6542: 65421J-1
[21] Bagayev S N, Bozhkov V G, Zakharyash V F, et al. Application of Schottky diodes as frequency converters in submillimetre and IR systems. Quantum Electron, 1998, 28: 542
[22] Huang T S, Fang R S. Barrier height enhancement of Pt/n-InP Schottky diodes by $P_2S_5/(NH_4)_2S$ solution treatment of the InP surface. Solid-State Electron, 1994, 37: 1461
[23] Kamimura K, Suzuki T, Kunioka A. InP metal–insulated– semiconductor Schottky contacts using surface oxide layers prepared with bromine water. J Appl Phys, 1980, 51: 4905
[24] Wada O, Majerfeld A, Robson P N. InP Schottky contacts with increased barrier height. Solid-State Electron,1982, 25: 381
[25] Lee Y S, Anderson W A. High-barrier height metal-insulator-semiconductor diodes on n-InP. J Appl Phys, 1989, 65: 4051
[26] Trt A, Yalcin N, Saglam M. Parameter extraction from non-ideal $C$–$V$ characteristics of a Schottky diode with and without interfacial layer. Solid-State Electron, 1992, 35: 835
[27] Aboelfotoh M O. Influence of thin interfacial silicon oxide layers on the Schottky-barrier behavior of Ti on Si(100). Phys Rev B, 1989, 39: 5070
[28] Ahaitouf A, Losson E, Bath A. On the determination of interface state density in n-InP Schottky structures by current–voltage measurements: comparison with DLTS results. Solid-State Electron, 2000, 44: 515